Journal of Functional Foods 92 (2022) 105044

Contents lists available at ScienceDirect

Journal of Functional Foods

journal homepage: www.elsevier.com/locate/jff

Anti-inflammatory effect of lentil hull (*Lens culinaris*) extract via MAPK/NF-κB signaling pathways and effects of digestive products on intestinal barrier and inflammation in Caco-2 and Raw264.7 co-culture

Li Peng [a,1], Fanghua Guo [a,1], Minjia Pei [a], Rong Tsao [b], Xiaoya Wang [c], Li Jiang [c], Yong Sun [a,*], Hua Xiong [a,*]

[a] State Key Laboratory of Food Science and Technology, Nanchang University, Nanchang 330047, Jiangxi, China
[b] Guelph Research and Development Centre, Agricultural and Agri-Food Canada, 93 Stone Road West, Guelph, ON N1G 5C9, Canada
[c] Jiangxi University of Traditional Chinese Medicine, Nanchang 330004, Jiangxi, China

ARTICLE INFO

Keywords:
Lentil hulls
Anti-inflammatory
In vitro digestion
Caco-2/RAW264.7 cell co-culture
Polyphenols

ABSTRACT

The polyphenol-rich lentil hulls are the by-product of lentils hulling process. In this manuscript, *in vitro* digestion, Caco-2 cell monolayer and Caco-2/RAW264.7 cell co-culture model were established to explore their anti-inflammatory mechanism, absorption of digestive products (RLD), and impact on the intestinal barrier. Results shown that high dose RLE and GLE could significantly inhibit the secretion of NO (30.23% and 31.08%, respectively), IL-6 (81.48% and 56.82%, respectively) and IL-1β (88.05% and 91.67%, respectively), and down-regulate the protein and mRNA expression of iNOS (56.46% and 45.69%, respectively) and COX-2 (76.53% and 46.65%, respectively), and inhibit the activation of MAPK and NF-κB signaling pathways. Polyphenols can be released from lentil hulls and protocatechuic acid glycoside derivative has the highest content (2205.09 ± 7.02 μg/g DW). Digestive products can be absorbed by intestine to maintain intestinal barrier and play anti-inflammatory effect. Above all, lentil hulls may be a potentially valuable functional dietary resource.

1. Introduction

Inflammation, an immune response caused by harmful external stimuli (i.e. infection, tissue damage), is usually manifested as redness, fever, pain, dysfunction and other symptoms at the inflammation site (Maleki, Crespo, & Cabanillas, 2019). During the inflammatory response, macrophage plays an important role in the formation of inflammatory mediators and pro-inflammatory cytokines, such as nitric oxide (NO) and prostaglandin E2 (PGE2), which are regulated by nitric oxide synthase (iNOS) and cyclooxygenase (COX-2), respectively (Villela-Castrejón, Antunes-Ricardo, & Gutiérrez-Uribe, 2017). Excessive production of proinflammatory mediators can lead to a variety of diseases, such as atherosclerosis, diabetes, obesity and cancer (Liu et al., 2019).

NF-κB (nuclear factor-kappa-light-chain-enhancer of activated B cells) and MAPKs (mitogen-activated protein kinases), two classical signaling pathways, are involved in the regulation of body inflammation (Z.-B. CHEN et al., 2020). NF-κB, an important transcriptional regulator, usually binds to its inhibitory protein (IκB) in the form of p50-p65 heterodimer, and exists in the cytoplasm in an inactive state (Kim & Bae, 2010). Phosphorylation and degradation of IκB will cause NF-κB to be activated and transferred to the nucleus, which induces the expression of multiple cytokines and participates in inflammatory responses (X. Wang et al., 2020). MAPKs is a family of serine/threonine protein kinases, including three major subfamilies: c-Jun N-terminal kinase (JNK), extracellular signal-regulated kinase 1/2 (ERK1/2) and p38

Abbreviations: RLE, red lentil hulls extract; GLE, green lentil hulls extract; RLD, red lentil hulls digestion product; TPC, total phenolic content; TFC, total flavonoid content; GAE, gallic acid equivalent; IN part, digestion product sediment; OUT part, digestive product supernatant; NO, nitric oxide; LPS, lipopolysaccharides; iNOS, inducible nitric oxide synthase; PEG2, prostaglandin E2; IL-6, interleukin-6; IL-1β, interleukin-1β; IL-8, interleukin-8; TNF-α, tumor necrosis factor-α; COX-2, cyclooxygenase-2; NF-κB, nuclear factor-kappa B; IκBα, inhibitor of NF-κB; MAPK, mitogen-activated protein kinase; JNK, c-jun N-terminal kinase; ERK, extracellular signal-regulated kinase.

* Corresponding authors.
E-mail addresses: yongsun@ncu.edu.cn (Y. Sun), huaxiong100@126.com (H. Xiong).
[1] These authors contributed equally to the manuscript and are co-first authors.

https://doi.org/10.1016/j.jff.2022.105044
Received 13 December 2021; Received in revised form 12 March 2022; Accepted 22 March 2022
Available online 1 April 2022

MAPK, which mediate basic biological processes and cell responses to external stress signals (Kaminska, 2005; Li et al., 2020). MAPKs can be phosphorylated and activate other kinases or nuclear proteins (Han et al., 2017). P38 MAPK plays a crucial role in the regulation of the expression of inflammatory factors, adhesion factors and chemokines (Ellen Herlaar & Brown, 1999; Zhou et al., 2020). Many studies have shown that polyphenols can down-regulate the secretion of inflammatory mediators (NO and PGE2) and pro-inflammatory factors (IL-6, IL-1β, and TNF-α) in the LPS-induced RAW264.7 cell inflammation model (Fang, Chen, Chen, Lin, & Fang, 2012; Wang, Li, Ge, & Lin, 2020), which are related to MAPKs and NF-κB signaling pathway (Feng et al., 2021).

Currently, the differentiated Caco-2 cell monolayer model has been widely used to study the absorption, transport and metabolism of dietary phytochemicals (Marina, Amin, Loh, Fadhilah, & Kartinee, 2019; Sadeghi Ekbatan et al., 2018; WEIGUANG YI, CASIMIR C. AKOH, JOAN FISCHER, & KREWER, 2006). In addition, it can be used to investigate the barrier function of intestinal epithelial cells, including the polarity of the intestinal epithelium and the permeability associated with tight junctions (TJs, a kind of protein complex) (Maren Amasheh et al., 2008; Noda, Tanabe, & Suzuki, 2012; Omonijo et al., 2019). While, the co-culture can simulate the microenvironment in vivo, which makes up for the deficiency of simulated physiological environment in monolayer cell culture to some extent. Co-culture of intestinal epithelial cells and immune cells is an important and powerful means to study their interaction mechanism (X. Hu et al., 2020).

Lentils (*Lens culinaris*), a staple food in North America, are native to India, which are widely grown in Canada, India, Australia, the United States, China, Ethiopia, the Mediterranean and Southeast Asia, among which Canada is the world's largest producer and exporter of lentils (Portman et al., 2020). As a by-product of lentil processing, lentil hulls are usually discarded as waste or used as animal feed (Zhong, Fang, Wahlqvist, & Wu, 2018). Lentil hulls are rich in dietary fiber and phytochemicals that have anti-inflammatory, antioxidant, and lower blood pressure, cholesterol, and blood sugar properties (Duenas, Hernandez, & Estrella, 2006). Studies have shown that the seed coat of legumes contains phenolic compounds with flavonoid structure, which are important natural antioxidants (Oomah, Caspar, Malcolmson, & Bellido, 2011; Troszyńska, Estrella, López-Amóres, & Hernández, 2002). Yeo and Shahidi (2020) identified the soluble phenols in lentil hulls with HPLC-ESI-MS/MS, mainly including phenolic acids, flavonoids and anthocyanins, which shows strong antioxidant capacity *in vitro*. However, the current researches on lentil hulls are mostly focused on the identification of phenolic composition and antioxidant activity *in vitro*; the anti-inflammatory activity of lentil hulls polyphenol extract in RAW264.7 cells, and the absorption and metabolism of polyphenols in lentil hulls after *in vitro* digestion and its anti-inflammatory activity have not been studied in Caco-2/RAW264.7 cell co-culture. In actual consumption, lentil hulls are directly ingested instead of extracts. The influence of food matrix on the release of polyphenols in lentil hulls cannot be ignored during the digestion process.

The composition and antioxidant capacity of polyphenols in red and green lentil hulls have been studied in our previous research (Minjia, Xiaoya, Hua, Fengxin, & Yong, 2021). In this study, the LPS-induced RAW264.7 cell inflammation model was established to study the anti-inflammatory activity and mechanisms of RLE and GLE; and *in vitro* digestion, Caco-2 cell monolayer and Caco-2/RAW264.7 cell co-culture model were used to explore the release of lentil hull polyphenols during digestion, the absorption of digested products and their effects on intestinal inflammation and intestinal barrier.

2. Materials and methods

2.1. Materials and reagents

The red and green lentil hulls (ADM Red Lentil Hulls and ADM Eston Green Lentil Hulls) were presented by the Research and Development Center of Guelph Agriculture and Agrofood (Canada). RAW264.7 cells and Caco-2 cells were purchased from the cell bank of the Institute of Chinese Academy of Sciences (Shanghai, China). Dulbecco's modified Eagle's medium (DMEM), phosphate buffered saline (PBS), Hank's balanced salt solution (HBSS), Cell Counting Kit-8 (CCK-8) and SDS-PAGE gel electrophoresis kit were purchased from Beijing Solarbio Technology Co., Ltd (Beijing, China). Lipopolysaccharides (LPS) was acquired from Sigma (St. Louis, MO, USA). Fetal bovine serum (FBS) was purchased from Biological Industries biotech company (Israel). NO detection kit was purchased from Beyotime Biotechnology (Shanghai, China). The TNF-α, IL-6, IL-1β and IL-8 ELISA kits were purchased from Thermo Fisher Scientific (Massachusetts, USA). Anti-p38/p-p38, IκBα/p-IκBα, NF-κB p65/p-p65 were obtained from Cell Signaling Technology (CST, MA, USA). Anti-iNOS, COX-2 and GAPDH were acquired from Beijing Absin Biotechnology Co., Ltd (Beijing, China). The RNA reverse transcription kit and RT-PCR quantitative kit were purchased from Takara Biotechnology Co., Ltd (Japan). Transwell plates (Model 3450; 24 mm diameter inserts; 0.4 μm pore size; 6 well plate) were acquired from Corning (Kennebunk, ME, USA).

2.2. Sample preparation

The RLE and GLE were prepared according to Guo et al. (2019). The 80% methanol (w/v) extracts of ADM Red Lentil Hulls and ADM Eston Green Lentil Hulls were denoted as RLE and GLE, respectively. The two crude lentil hull extracts were purified by solid phase extraction (SPE) columns (Oasis HLB 6cc, Waters). Briefly, the RLE and GLE were weighed and dissolved in an appropriate amount of ultrapure water. The SPE column was activated with 6 mL methanol and water, respectively, and then the sample solution was passed through the SPE column. The adsorbed polyphenols were eluted with methanol and the filtrate was collected, then rotary evaporated and freeze-dried. And the purified product was used in subsequent cell experiments.

2.3. In vitro digestion

The ADM Red Lentil Hulls were subjected to *in vitro* digestion and the digestion process was referred to Brodkorb et al. (2019). The digestion reserve solution was prepared according to Table S1.

Oral digestion stage: 3 g ADM Red Lentil Hulls were moistened with 2 mL ultrapure water, and 4 mL SSF solution contained α-amylase (75 U/mL) and $CaCl_2(H_2O)_2$ were added. Adjusted the pH to 7.0, and then added ultrapure water until the system reach 10 mL. It was shaken at 37 ℃, 300 rpm/min for 5 min.

Gastric digestion stage: added 8 mL SGF solution contained pepsin (2000 U/mL) into the oral digestion product, adjusted the pH to 3.0 with 1 mol/L HCl solution, and then added ultrapure water to make the system reach 20 mL. It was shaken at 37 ℃, 100 rpm/min for 2 h.

Intestine digestion stage: added 16 mL SIF solution contained pancreatin (100 U/mL) and bile salt (10 mM) into the gastric digestion product, adjusted the pH to 7.0 with 1 mol/L NaOH, and then added ultrapure water to make the system reach 40 mL. The system was shaken at 37 °C, 100 rpm/min for 2 h.

For each digestion stage, the supernatant was denoted as OUT part; and the residue was extracted with 80% methanol and was denoted as IN part. The OUT part of the intestinal digestion stage was purified by SPE columns, and was labeled as RLD for cell experiments. The purified OUT part was used for UPLC analysis. Samples were flushed with N_2 during the digestion at the stomach and small intestine stages to remove the influence of oxygen. All experiments were performed in triplicate.

2.4. Total phenolic content (TPC) and total flavonoid content (TFC)

The TPC and TFC in the IN and OUT part were determined according to our previous research (Y. Sun et al., 2020; Yong Sun et al., 2015).

2.5. Antioxidant assays

The antioxidant activities of the sample were determined by the DPPH, ABTS and FRAP assays.

DPPH assay. The measurement of DPPH radical scavenging ability was based on the method of B. Zhang et al. (2014) with a slight modification. In brief, 280 μL 65 μmol/L DPPH solution was added to the 96-well plate, then add 20 μL sample or Trolox standard solution with different concentrations. The absorbance was measured at 540 nm after 30 min reaction at room temperature under dark conditions. All measurements were performed in triplicate, and the results were expressed as Trolox equivalent per gram of dry weight of lentil hulls (μmol Trolox/g DW).

ABTS assay. The ABTS assay was measured using the total antioxidant capacity test kit (Beyotime Biotechnology, Shanghai, China) according to the manufacturer's instructions. The results were expressed as Trolox equivalent per gram of dry weight of lentil hulls (μmol Trolox/g DW).

FRAP assay. The FRAP assay was measured using kit (Beyotime Biotechnology, Shanghai, China) according to the manufacturer's instructions. The results were expressed as $FeSO_4$ equivalent per gram of dry weight of lentil hulls (mmol $FeSO_4$/g DW).

2.6. Quantitative analysis by UPLC

Chromatographic separation adopts UPLC system (Agilent 1290 Infinity UPLC system). A Waters ACQUITY UPLC® BEH C18 1.7 μm 2.1 × 100 mm Column (Waters, USA) was used for detection. The mobile phase A was 0.1% formic acid–water (v/v), and the mobile phase B was 0.1% formic acid-acetonitrile (v/v). The gradient elution procedure was: 0–5 min, 5% B; 5–21 min, 5%-21% B; 21–22 min, 21%-55% B; 22–25 min, 55% B; 25–35 min, 55%-100% B. The flow rate and injection volume were 0.3 mL/min and 3 μL, respectively.

2.7. UPLC-LTQ-Orbitrap-MS/MS

Liquid chromatographic conditions. Chromatographic separation adopts UPLC system (Thermo Accela 600 UPLC system, Thermo Scientific, Bremen, Germany). A Waters ACQUITY UPLC® BEH C_{18} 1.7 μm 2.1 × 100 mm Column (Waters, USA) was used for detection. The mobile phase A was 0.1% formic acid–water (v/v), and the mobile phase B was 0.1% formic acid-acetonitrile (v/v). The gradient elution procedure was: 0–2 min, 5% B; 2–9 min, 5%-21% B; 9–16 min, 21%-29% B; 16–22 min, 29%-55% B; 22–25 min, 55% B; 25–35 min, 55%-100% B; 35–35.1 min, 100%-5% B; 35.1–38 min, 5% B. The flow rate and injection volume were 0.3 mL/min and 3 μL, respectively. The column temperature was 25 ℃. The detection wavelength was set at 280 and 320 nm.

Mass spectrometric conditions. Mass spectrometry was performed by a linear ion trap quadrupole orbit mass spectrometer (LTQ-Orbitrap MS), which equipped with heated electrospray ion source (HESI-II; Thermo Fisher Scientific; USA). The measurement was performed in negative ion mode. The best mass spectrometry parameters were as follows: source voltage: 5 kV, capillary temperature: 275℃, sheath gas flow rate: 42 arb; auxiliary gas (N_2) flow rate: 11 arb. The mass spectrometry data were collected in the whole range of 100–1500 *m/z*. The Xcalibur v.2.0 software (Thermo Fisher, San Jose, CA, USA) and Qualbrowser were used for data collection and processing.

2.8. Cell culture and viability

RAW264.7 cells and Caco-2 cells were cultured in DMEM medium (containing 10% FBS and 1% penicillin–streptomycin) at 37℃ and 5% CO_2. Cell viability was measured with CCK-8 kit. CCK-8 is a rapid and highly sensitive detection reagent based on WST-8 (2-(2-Methoxy-4-nitrophenyl)-3-(4-nitrophenyl)-5-(2,4-disulfobenzene)-2H-tetrazolium monosodium salt) that is widely used in cell proliferation and cytotoxicity. WST-8 is reduced to a highly water-soluble orange-yellow formazan product by dehydrogenases in mitochondria in the presence of an electron carrier (1-Methoxy PMS). And for the same cell, the depth of the color is proportional to the number of living cells. Briefly, 2×10^4 cells were laid in 96-well plate, and 100 μL of sample with different co ncentrations (10, 25, 50, 100, 150, 200, 250, 300 μg/mL) were added to each well after culturing for 12–18 h. Them, 10 μL CCK-8 reagent was added to each well for 1 h, and the absorbance value was measured at 450 nm. Each group was done in six parallels.

2.9. LPS-stimulated RAW264.7 cell inflammation model

RAW264.7 cells were inoculated in a 24-well plate with 5×10^5 cells/well, and the culture medium was discarded after incubation for 12–18 h. The experimental group was added with 1 mL DMEM contained 1 μg/mL LPS and RLE or GLE (50, 100, 200 μg/mL); the positive control group was added with 1 mL DMEM contained 1 μg/mL LPS (from Escherichia coli O55:B5, purufied by phenol extraction); and the blank control group was added with 1 mL DMEM. Each group was provided with three multiple wells. After cultured for 24 h, the supernatant medium and cells were collected.

2.10. Caco-2 cell monolayer model

The Caco-2 cells were inoculated to AP side of Transwell plate at a density of 3×10^5 cells /mL, and the addition volume was 1.5 mL; 2.6 mL DMEM (with 10% FBS) was added to BL side. The medium was changed every two days and the transepithelial electrical resistance (TEER) value was measured with the Millicell ERS voltammeter (Millipore, Bedford, MA, USA). Generally, after culturing for about 21 days, the cells differentiate completely and form a dense monolayer membrane.

The transmembrane flux of fluorescein sodium was measured. The Caco-2 cell monolayer cultured for 21 days was washed with HBSS preheated at 37 °C, and equilibrated at 37 °C and 5% CO_2 for 30 min. Then 1.5 mL fluorescein sodium solution (100 μg/mL) was added to the AP side, and 2.6 mL HBSS solution was added to BL side. The liquid on BL side was taken at 0.5 h, 1 h and 2 h, respectively. The fluorescence intensity was measured under the conditions of excitation wavelength 427 nm and emission wavelength 536 nm. The apparent permeability coefficient (Papp) was calculated using the following formula.

$$Papp = \triangle Q / (\triangle t \times A \times C_0).$$

$\triangle Q$: the passage amount of fluorescein sodium in $\triangle t$ period; A: the monolayer area (cm^2); C_0: the initial concentration of fluorescein sodium on AP side (μg/mL).

2.11. Absorption of RLD in Caco-2 cell monolayer

The Caco-2 cell monolayer was washed three times with HBSS preheated at 37℃, and was equilibrated at 37℃ and 5% CO_2 for 2 h. Then 1.5 mL 150 μg/mL RLD (dissolved in DMEM at pH 6.5) was added to AP side, and 2.6 mL DMEM was added to BL side. The culture medium on BL side was collected at 0 h, 2 h, 6 h and 24 h, and purified by SPE column for UHPLC-LTQ-Orbitrap-MS/MS analysis. And Caco-2 cells were collected for Western blot.

2.12. Caco-2/RAW264.7 cell co-culture model

RAW264.7 cells were inoculated in a 6-well plate at a density of 2×10^6 cells/well and cultured for 12 h. Then Transwell chambers with Caco-2 monolayers cultured for 21 days were transferred to the six-well plate containing RAW264.7 cells and balanced for 24 h at 37℃ and 5% CO_2. The blank group and LPS group were added 1.5 mL pH 6.5 DMEM medium on the AP side, and the RLD group was added 1.5 mL 150 μg/

mL RLD solution on the AP side; and all three groups were added with 2.6 mL DMEM medium at BL side. After cultured for 6 h, LPS was added to the BL side of the LPS group and RLD group to make its final concentration be 1 μg/mL. Cells and supernatants were collected for analysis after cultured for another 12 h.

2.13. NO, IL-6, IL-8, IL-1β and TNF-α determination

NO, IL-6, IL-8, IL-1β and TNF-α contents were determined according to the instructions of the corresponding kit.

2.14. Real-Time PCR

The total RNA was extracted using the RNAeasy™ animal RNA extraction kit, and the concentration and purity was determined. The total RNA was used as the template to reverse transcribe RNA into cDNA using the reverse transcription kit. The fluorescence quantitative reaction was performed according to the instructions of the TBGreen® Premix Ex Taq™ quantitative PCR kit. The parameters of the reaction procedure were as follows: pre-denaturation at 95℃ for 30 s, 95℃ for 5 s, 60℃ for 30 s, PCR for 39 cycles, 65℃ for 5 s, 95℃ for 50 s. The primer sequences of each gene were shown in Table S2.

2.15. Western blot analysis

The concentrations of extracted proteins were determined with BCA protein kit (Solarbio Science, Beijing, China). The proteins were separated by SDS-PAGE gel electrophoresis, and transferred to PVDF membrane using WB electrotransfer device. Then the PVDF membrane was sealed with Quickblock solution (Beyotime Biotechnology, China) at room temperature for 1 h. The primary antibody was incubated at room temperature for 1 h and then at 4 ℃ overnight. The primary antibody was washed away with TBST, and the secondary antibody was incubated for 1.5 h at room temperature. Enhanced chemiluminescence detection system (BIO-RAD, USA) was used to detect protein bands. GAPDH was used as internal reference, and the corresponding protein expression was calculated using Image J software.

2.16. NF-κB p65 nuclear metastasis

RAW264.7 cells were added to a 6-well plate (1×10^6 cells/well) containing 25 × 25 mm glass sheets, and incubated overnight at 37 °C and 5% CO_2. The experimental group was added with 1 mL 1 μg/mL LPS and 200 μg/mL RLE or GLE; the positive control group was added with 1 mL 1 μg/mL LPS; the blank group was added with the same amount of DMEM; all group cultured for 24 h. After fixed with 4%

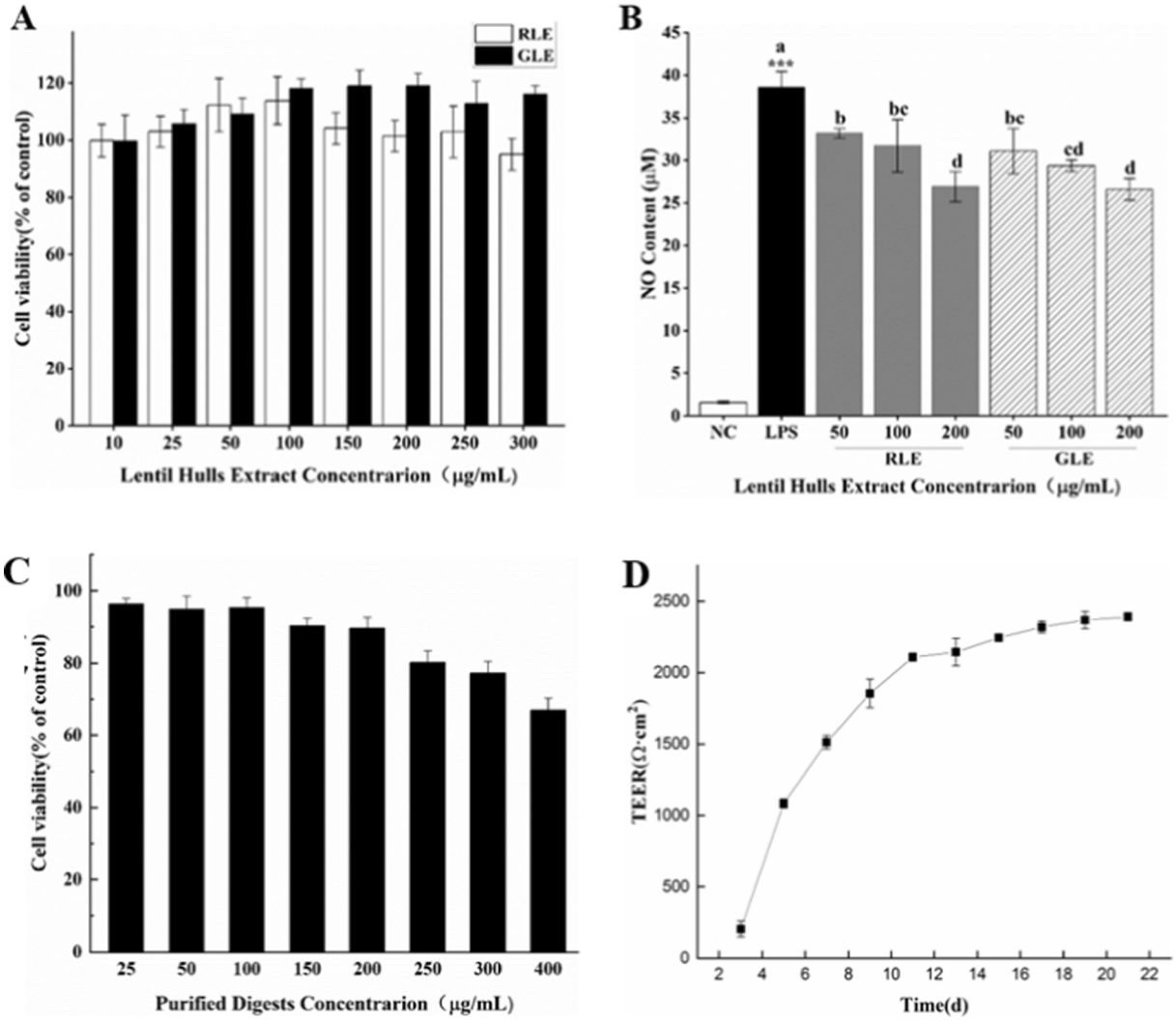

Fig. 1. Effect of RLE and GLE on cell viability (A) and NO production (B) in LPS-stimulated RAW264.7 cells, n = 6; effect of RLD on Caco-2 cell viability (C), n = 6; TEER values of Caco-2 cell monolayer (D), n = 3. The results were expressed as mean ± SD, *: indicated the significant difference between the NC and LPS group, ***: $P < 0.001$. Different letters represent significant difference between LPS and experimental group ($P < 0.05$).

paraformaldehyde solution at 4 ℃ for 30 min, cells were washed with PBS. Then the cells were blocked with 5% BSA for 30 min at room temperature, and incubated with NF-κB p65 antibody (1:100) at 4 ℃ overnight. The results were detected by laser confocal microscope.

2.17. Statistical analysis

The results were expressed as mean ± standard deviation (mean ± SD). SPSS (version 20.0, IBM, USA) was used for univariate ANOVA analysis of the experimental data. $P < 0.05$ indicated that there was a significant difference between the data in each group.

3. Results

3.1. Effect of RLE and GLE on cell viability and NO secretion of RAW264.7 cells

The CCK-8 kit was used to determine the effects of RLE and GLE on RAW264.7 cells viability. As shown in Fig. 1A, RLE and GLE had no toxic effect on RAW264.7 cells at 10–250 and 10–300 ug/mL, respectively. Therefore, 50, 100, and 200 μg/mL were selected for subsequent experiments.

As shown in Fig. 1B, under the stimulation of LPS, the NO content of the positive control group (LPS group) was increased significantly ($P < 0.001$), while RLE and GLE were significantly inhibited the release of NO in a dose dependent manner. At the concentration of 200 μg/mL, the inhibitory effects of the two kinds of lentil hull extracts were similar, reaching 30.23% and 31.08%, respectively. Studies have shown that the polyphenols in beans can effectively inhibit the release of NO (Mirali, Purves, & Vandenberg, 2017), which is consistent with our results.

3.2. Effect of RLE and GLE on iNOS and COX-2 protein and mRNA expression in LPS-stimulated RAW264.7 cells

As shown in Fig. 2A, B, D and E, compared with NC group, the protein expression of iNOS (1.08 ± 0.01) and COX-2 (1.86 ± 0.10) in RAW264.7 cells were significantly increased after stimulated by LPS ($P < 0.001$), while which were significantly ($P < 0.05$) down-regulated in a dose dependent manner after treated with RLE and GLE, and the effect of RLE was better than that of GLE. Treated 200 μg/mL RLE, the protein expression of iNOS and COX-2 was reduced by 56.46% and 76.53%, respectively. After LPS treatment, the mRNA expression of iNOS and COX-2 was significantly higher than that of NC group ($P < 0.001$); however, this result was reversed by all concentrations of RLE and GLE (Fig. 2C and F). The results showed that both RLE and GLE could significantly reduce the mRNA and protein expressions of iNOS and COX-2 in LPS-induced RAW264.7 cells, and the effect of RLE was better.

3.3. Effect of RLE and GLE on IL-6 and IL-1β production and mRNA expression in LPS-stimulated RAW264.7 cells

The effect of RLE and GLE on the mRNA expression and secretion of IL-6 and IL-1β in LPS-stimulated RAW264.7 cells were shown in Fig. 2G, H, I, and J. Compared with the NC group, the release and mRNA expression of IL-6 and IL-1β were increased significantly after LPS stimulation ($p < 0.001$). After RLE and GLE intervention, both the release and mRNA expression of IL-6 and IL-1β were reduced, especially at high doses (200 μg/mL). The results showed that both RLE and GLE could significantly reduce the IL-6 and IL-1β content to play an anti-inflammatory role in LPS-induced RAW264.7 cells, and the effect of RLE was better.

3.4. Effect of RLE and GLE on NF-κB/MAPK signaling pathway and nuclear transfer of NF-κB p65 in LPS-stimulated RAW264.7 cells

In order to further explore the anti-inflammatory effects and mechanisms of lentil hull extracts, MAPK and NF-κB signaling pathways were detected. As shown in Fig. 3A, and B, compared with the NC group (0.39 ± 0.01), the phosphorylation of p38 protein in RAW264.7 cells was significantly increased after LPS stimulation ($P < 0.001$). Nevertheless, both RLE and GLE could inhibit the p38 phosphorylation, and the inhibitory effect of RLE was concentration-dependent, while GLE had the best effect (29.06%) at 100 μg/mL. The expression of NF-κB signaling pathway related proteins (IκBα and p65) were shown in Fig. 3C and D. Compared with the NC group, the expression of p-IκBα and p-p65 in LPS-stimulated RAW264.7 cells were increased significantly, reaching 0.60 ± 0.02 and 0.70 ± 0.00, respectively ($P < 0.001$). While RLE and GLE significantly down-regulated the expression of p-IκBα and p-p65 ($P < 0.05$), in which 200 μg/mL RLE and GLE had the best inhibitory effect on p-IκBα (62.68%) and p-P65 (30.76%), respectively.

NF-κB P65 is widely present in the cytoplasm of normal cells, which is transferred to the nucleus and initiates the transcription of inflammation-related genes after stimulation by inflammatory factors. The increase of p65 nuclear translocation is an important marker of inflammatory response. As shown in Fig. 3E and F, after treatment of 200 μg/mL RLE and GLE, the nuclear metastasis of NF-κB p65 was significantly reduced (48.81% and 44.36%) compared with the LPS group, which may be related to the decrease of p-IκBα.

Lentil hull extract exerted a good anti-inflammatory activity through inhibition of MAPK and NF-κB signaling pathways, which may be related to the rich phenolic substances in the extract. In fact, lentil hulls are consumed directly in the diet instead of their extracts, and they have to undergo complex intestinal digestion. Food matrix affects the release and bioavailability of polyphenols. Studies have shown that dietary fiber binds to polyphenols either covalently or non-covalently (Jakobek & Matić, 2019; Quirós-Sauceda et al., 2014). Therefore, *in vitro* digestion and co-culture models were established to investigate the digestive fate of lentil hull (polyphenols) and the effects of their digestive products on intestinal barrier and inflammation. Red lentil hulls with better anti-inflammatory effects were used for further research.

3.5. Effect of in vitro digestion on the TPC, TFC and antioxidant capacity of red lentil hulls

The TPC and TFC in digestion products of red lentil hulls were shown in Fig. 4A and B. As the digestion progresses, TPC and TFC were increased, indicating that polyphenols can be released from the lentil hulls, and their contents were higher than the free and bound TPC (8.32 ± 0.24 and 3.68 ± 0.05 mg GAE/g DW) and TFC (5.28 ± 0.49 and 2.87 ± 0.05 mg CAE/g DW) of lentil hull reported in our previous study (Minjia et al., 2021). Interestingly, the TPC and TFC remaining in the lentil hull had the highest content after the gastric digestion, which may be due to pepsin hydrolyzing the protein in lentil hull and making the polyphenols easier to extract. And the changes of antioxidant capacity were shown in Fig. 4C, D and E. During digestion, the antioxidant capacity (DPPH, FRAP and ABTS) of digestive juices (OUT part) were increased, which was consistent with the continuous release of polyphenols. However, the antioxidant capacity of the IN part was gradually decreased during the digestion process.

3.6. Changes of main phenolic substances in red lentil hull during in vitro digestion

In our previous studies, polyphenols in red lentil hull were only qualitatively analyzed (Minjia et al., 2021). The contents of major polyphenols during digestion were quantitatively analyzed in order to determine the effect of digestion on the release of polyphenols (Fig. 5A and Table 1). As shown in Table 1, coumaric acid derivative (peak 1) and isorhamnetin-7-O-glucoside (peak 4) were mainly released in the mouth and small intestine; while soybean phenol E glycoside derivative (peak 5) was not released during oral digestion, but was released in large quantities during gastric digestion, reaching 240.81 ± 0.22 μg/g DW;

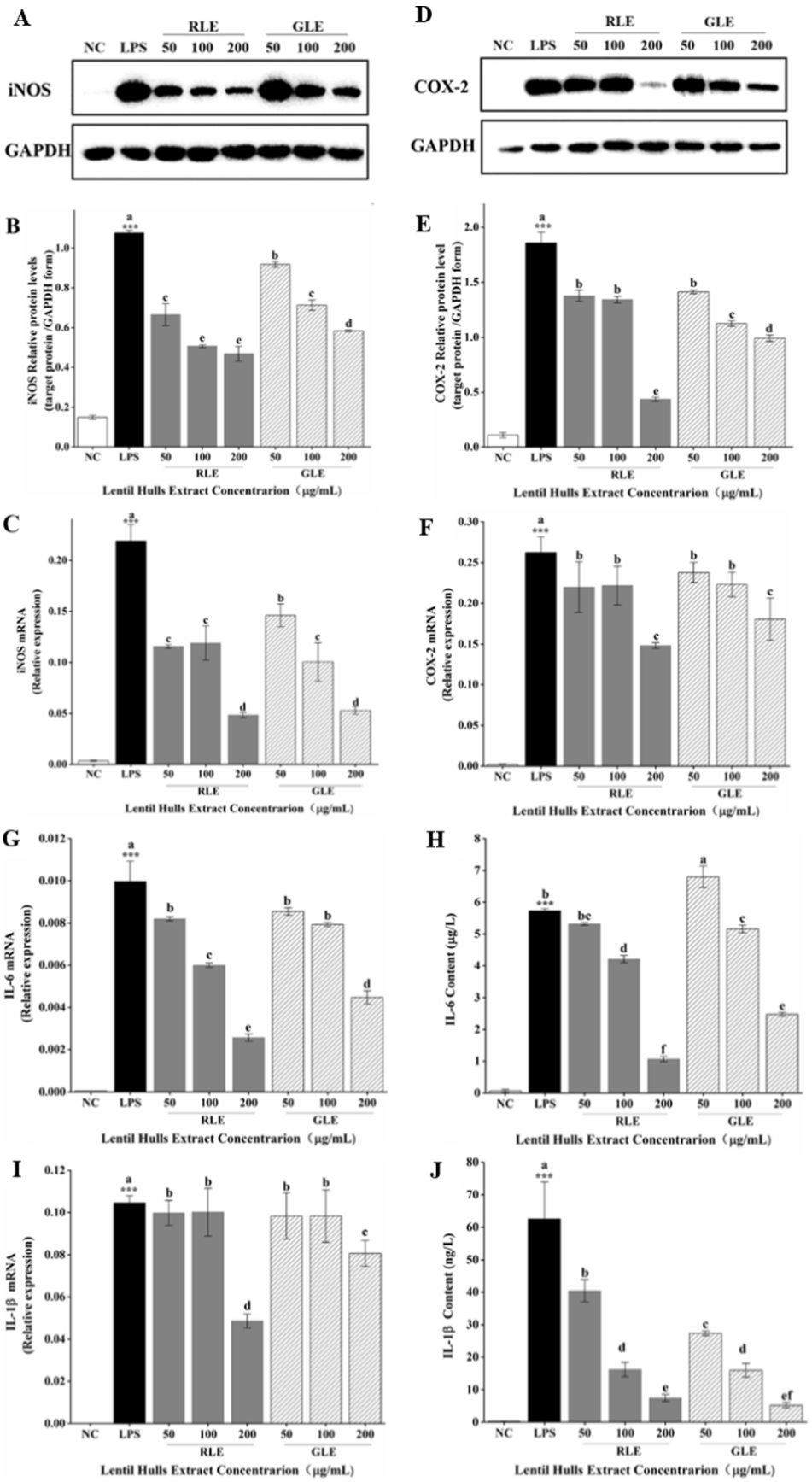

Fig. 2. Effect of RLE and GLE on iNOS, COX-2, IL-6, and IL-1β in LPS-stimulated RAW264.7 cells. RAW264.7 cells were cultured for 12–18 h, then LPS (the final concentration: 1 μg/mL) and samples with different concentrations were added for another 24 h. The results were expressed as mean ± SD, n = 3. *: indicated the significant difference between the NC and LPS group, ***: $P < 0.001$. Different letters represent significant difference between the LPS and experimental group ($P < 0.05$).

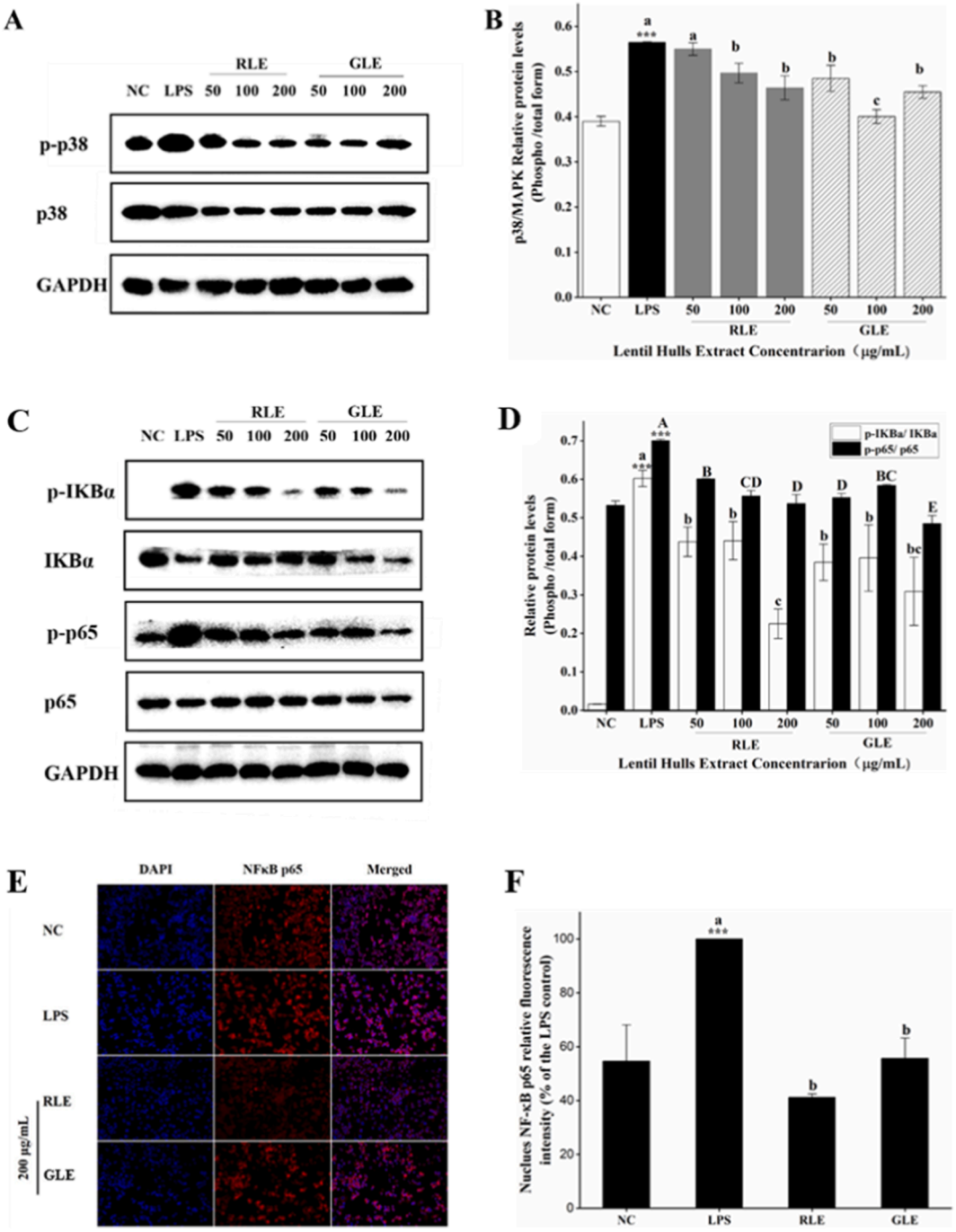

Fig. 3. Effect of RLE and GLE on NF-κB/MAPK signaling pathway and nuclear transfer of NF-κB p65 in LPS-stimulated RAW264.7 cells. RAW264.7 cells were cultured for 12–18 h, then LPS (the final concentration: 1 μg/mL) and samples with different concentrations were added for another 24 h. The results were expressed as mean ± SD, n = 3. *: indicated the significant difference between the NC and LPS group, ***: $P < 0.001$. Different letters represent significant difference between the LPS and experimental group ($P < 0.05$).

peaks 2 was identified as protocatechuic acid glycoside derivative, which was released in small amounts in the mouth and stomach, mainly in the small intestine, reaching 2205.09 ± 7.02 μg/g DW, and was the most abundant polyphenols; and interestingly, kaempferol tetraglucoside (peak 3) was released in large quantities during oral digestion. In general, as the digestion progresses, the content of polyphenols were continued to increase (OUT part), suggesting that enzymes in the digestive tract (amylase, protease, and trypsin) may facilitate the release of polyphenols from red lentil hulls.

3.7. Caco-2 cell viability and evaluation of Caco-2 cell monolayer model

The CCK-8 method was used to determine the effects of RLD at different concentrations (25, 50, 100, 150, 200, 250, 300, 400 μg/mL) on Caco-2 cell viability. As shown in Fig. 1C, the survival rate of Caco-2 cell was lower than 90% at 200 μg/mL, and it was continuously decreasing with the increase of concentration. Therefore, 150 μg/mL was selected for subsequent experiments.

As shown in Fig. 1D, in the first 11 days, the cells were continued to differentiate and the TEER value increased rapidly; and it remained stable from the 19th day and reached 1924 ± 29 Ω cm^2 on the 21st day,

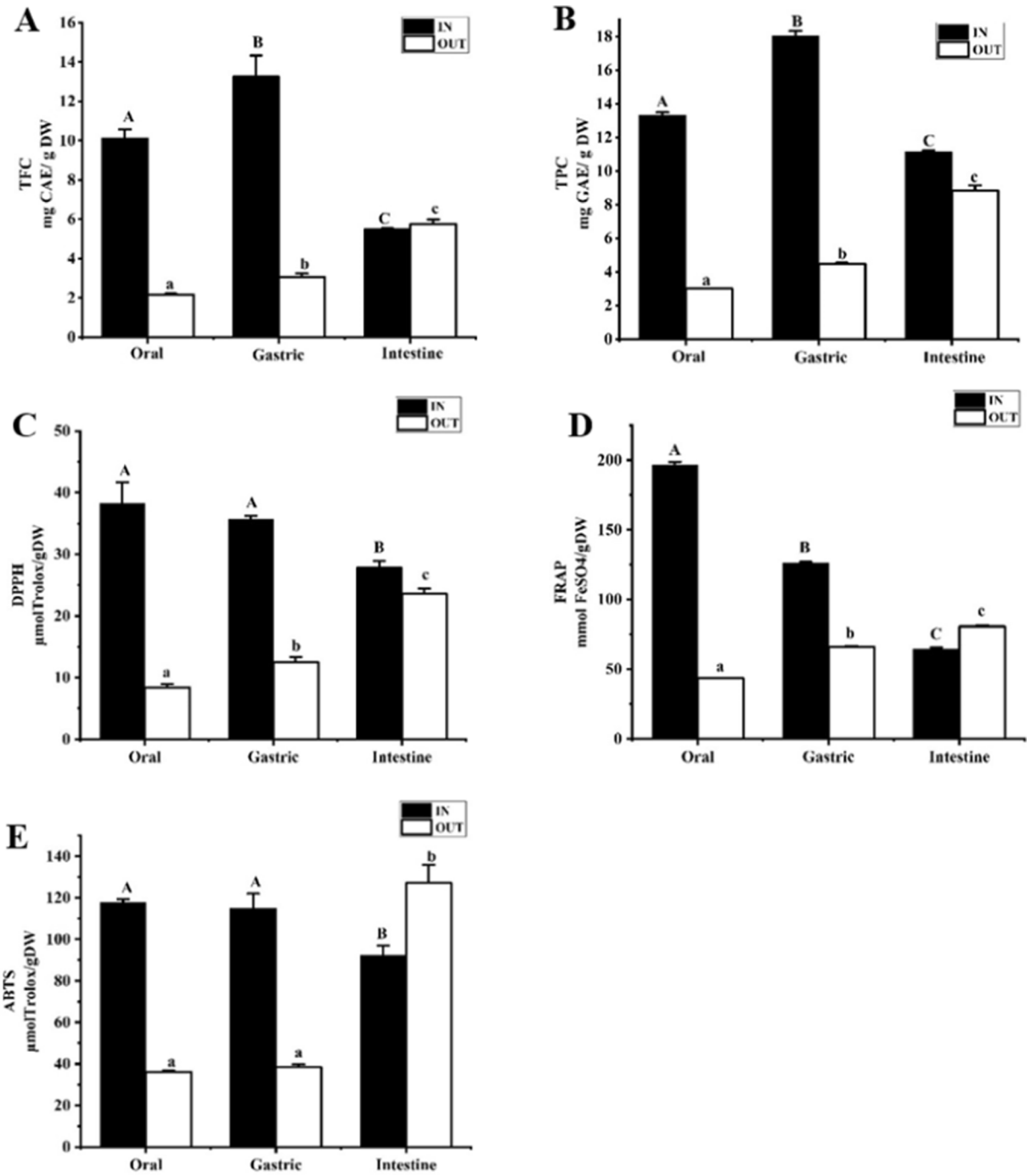

Fig. 4. TFC (A), TPC (B) and antioxidant capacity (C, D, E) of the IN and OUT parts of red lentil hull during *in vitro* digestion. Different letters represent significant difference ($P < 0.05$).

indicating that a complete and stable Caco-2 cell monolayer has been formed. On the other hand, sodium fluorescein was used to determine the permeability of Caco-2 cell monolayer. The Papp value of fluorescein sodium transported in Caco-2 cell monolayer for 2 h was $3.56 \pm 0.11 \times 10^{-7}$ cm/s, which was far below the critical value of 1×10^{-6} cm/s (Table S3). All these results indicated that the Caco-2 cells were tightly packed, and the permeability and integrity of the formed monolayer met the requirements after 21 days of culture.

3.8. Absorption and transportation of RLD and its effect on TJs

The absorption and transportation of RLD in the Caco-2 cell monolayer was shown in Fig. 5B, only kaempferol tetraglucoside was transported into the basolateral (BL) side, and the content was increased over time. Other digestive products were not be detected in the basolateral side. Meanwhile, the influence of RLD on tight junction protein expression were shown in Fig. 5C and D. After 6 h of culture, the expression of occludin protein was increased significantly ($P < 0.001$), and the protein of claudin-1 was increased slightly, indicating that the digestion product could promote the expression of tight junction protein. These results suggested that the digestive products of red lentil hull can be absorbed by the intestine and may play a role in improving the intestinal barrier function.

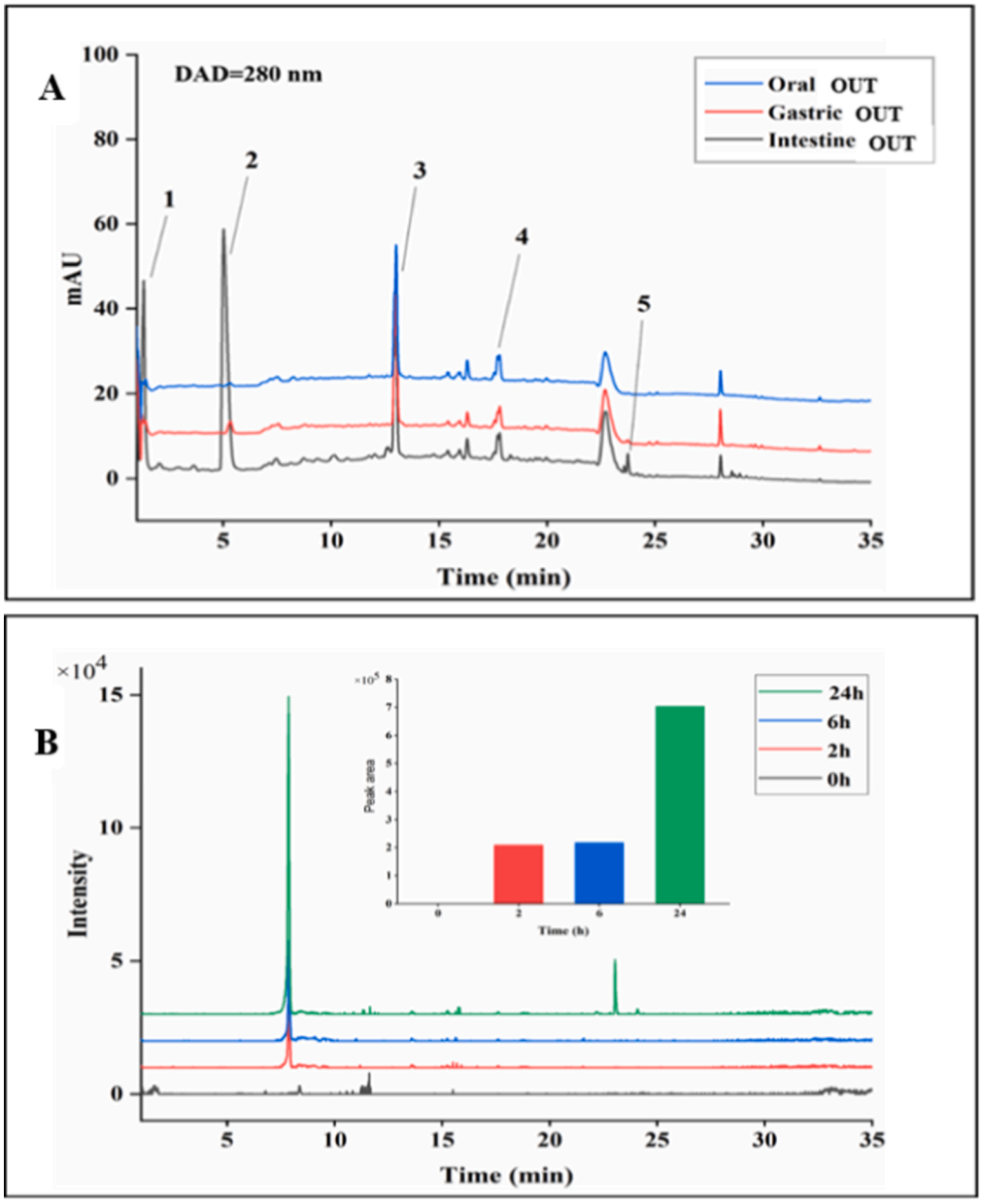

Fig. 5. UPLC chromatogram of major phenolics in the OUT parts of red lentil hull during *in vitro* digestion (A); TIC chromatogram of RLD absorption and transport at 0, 2, 6, and 24 h (B); Effects of RLD on tight junction proteins of Caco-2 cells monolayer (C, D). The results were expressed as mean ± SD, n = 3. *: indicated the significant difference between the NC and RLD group, ***: $P < 0.001$. (For interpretation of the references to color in this figure legend, the reader is referred to the web version of this article.)

Table 1
Changes of major phenolic compounds in the OUT part of red lentil hull during *in vitro* digestion.

Peak number	Phenolics	Standards	Content (μg/ g DW)		
			Oral	Gastric	Intestine
1	Coumaric acid derivative	Gallic acid	266.75 ± 0.42^{a}	268.28 ± 5.48^{a}	603.06 ± 33.83^{b}
2	Protocatechuic acid glycoside derivative	Protocatechuic acid	86.83 ± 2.87^{a}	141.74 ± 6.41^{b}	2205.09 ± 7.02^{c}
3	Kaempferol tetraglucoside	Kaempferol	674.67 ± 3.23^{a}	715.35 ± 10.07^{bc}	752.33 ± 28.55^{c}
4	Isorhamnetin-7-O-glucoside	Epicatechin	288.45 ± 8.34^{b}	278.69 ± 9.07^{b}	321.64 ± 7.28^{a}
5	Soybean phenol E glycoside derivative	Gallic acid	ND	240.81 ± 0.22^{a}	265.52 ± 2.77^{b}

ND: not detected. Different letters within the same line indicate significant difference ($P < 0.05$).

3.9. Effects of RLD on intestinal barrier and inflammation in Caco-2 /RAW264.7 co-culture

The effect of RLD on intestinal barrier and inflammation was shown in Fig. 6. After LPS treatment, the Papp value (Fig. 6A) was increased significantly and the expression of tight junction protein (Fig. 6B) was decreased compared with the normal group ($P < 0.05$), indicating that permeability of Caco-2 cells monolayer was increased and intestinal barrier was damaged. While RLD was decreased significantly the Papp value and restored intestinal tight junction (claudin-1 and ZO-1). On the other hand, digestive products can also relieve intestinal inflammation. As shown in Fig. 6E, F, G, and H, LPS added to the BL side could induce inflammation in Caco-2 cells and RAW264.7 cells, showing secrete a large amount of pro-inflammatory factor (TNF-α, IL-8, IL-1β, and IL-6), but they were inhibited after RLD treatment, especially TNF-α and IL-8 ($P < 0.05$). Interestingly, RLD had no significant effect on the increase of iNOS and COX-2 mRNA expression induced by LPS (Fig. 6C and D). These results indicated that polyphenol-rich RLD can improve inflammation-induced intestinal barrier dysfunction and be transported and absorbed to exert anti-inflammatory effects.

4. Discussion

Excessive inflammation is considered as the key factor of many diseases, such as cardiovascular disease, chronic inflammatory bowel disease and cancer (Kaminska, 2005). The LPS-induced RAW264.7 cell model is widely used to study anti-inflammatory effects and mechanisms (X. Hu et al., 2020). Hooshmand et al. (2015) showed that dried plum could significantly reduce the expression of COX-2 and iNOS induced by LPS, which was attributed to polyphenols in plum, a class of important natural antioxidants. In this study, similar results were found, showing that the contents of NO, iNOS and COX-2 were significantly reduced after RLE and GLE treatment. The rise of these inflammatory mediators will cause the expression of inflammatory factors and activate downstream inflammatory pathways (T. Y. Hu et al., 2019). RLE and GLE were able to reduce IL-6 and IL-1β levels, which can induce the release of NO and PGE2 and activate inflammatory signal pathways such as MAPK/NF-κB to induce and intensify the inflammatory response (Dinarello, 2011; Zelova & Hosek, 2013). These data suggested that RLE and GLE can alleviate LPS-induced inflammation, which may be related to the polyphenols in the extract identified in our previous study, contained 12 free phenols and 9 bound phenols (Minjia et al., 2021).

NF-κB signaling pathway is involved in mediating inflammatory response and metabolic regulation. The results shown that RLE and GLE significantly down-regulated the phosphorylation expression of IκBα and p65 protein, and attenuated the nuclear transfer of NF-κB p65 to inhibit the activation of NF-κB signaling pathway. Moreover, MAPK is also an important signaling pathway involved in inflammatory response, including ERK (involved in cell proliferation and differentiation), JNK (responsible for regulating apoptosis and stress response), and P38 (involved in inflammation and apoptosis) (Zhou et al., 2020). RLE and GLE can significantly inhibit the phosphorylation of p38 protein and the activation of MAPK signaling pathway. In general, the polyphenol-rich lentil hull extract can exert anti-inflammatory effects by inhibiting the MAPK and NF-κB signaling pathways and reducing the expression of inflammatory factors, and the effect of RLE was better than that of GLE.

However, whether these polyphenols in the lentil hull can be released, absorbed and transported and exert anti-inflammatory effects during the digestion process was still unknown. Therefore, the digestive fate of phenolic components in red lentil hull and the absorption and transport of digested products and their anti-inflammatory activities were further explored using *in vitro* digestion, Caco-2 cell monolayer, and Caco-2/RAW264.7 cell co-culture models. The results shown that the TPC and TFC in the OUT part were increased from oral to small intestine, indicated that polyphenols were continuously released from the lentil hull into the digestive juice, which was consistent with the changes of antioxidant capacity (DPPH, FRAP, and ABTS). Blancas-Benitez, Pérez-Jiménez, Montalvo-González, González-Aguilar, and Sáyago-Ayerdi (2018) showed that phenolic compounds released from guava fruit reached the highest value in intestinal digestion during *in vitro* digestion, which was similar to the results of this study. Among the digestive products, the five main released polyphenols were quantitatively analyzed, including protocatechuic acid glycoside derivative, kaempferol tetraglucoside, coumaric acid derivative, isorhamnetin-7-O-glucoside and soybean phenol E glycoside derivative, which were continuously released from the lentil hull as digestion progresses and were affected by various hydrolytic enzymes in the digestive tract.

The active substances are absorbed by the intestinal tract into the blood, and transported to the corresponding parts to play a specific role. The Caco-2 cell monolayer is a common model for studying intestinal absorption and transport. Among the digested products, only kaempferol tetraglucoside can be absorbed and transported, which may be related to their structure. Flavonoids with more glycosylation were demonstrated to be more readily transported across the Caco-2 monolayer (H. Zhang et al., 2020). And the transported content increased with time, indicating that it may enter the body as a bioactive component and play a role. Meanwhile, RLD can promote the expression of intercellular tight junction proteins (occludin and claudin-1), revealing that RLD may have a potential effect on improving intestinal barrier function. However, the absorption and transport mechanism of kaempferol tetraglucoside is unclear, which is our further research work.

Intestinal barrier dysfunction can lead to inflammatory bowel disease and colon cancer. Maintaining an appropriate level of tight junctions are the key to the treatment of inflammatory bowel disease (Bian et al., 2020; Omonijo et al., 2019). Studies have shown that plant polyphenols can improve intestinal barrier dysfunction (Sadeghi Ekbatan et al., 2018). Our results suggested that the polyphenol-rich digestive products of red lentil hull (RLD) can restore the mRNA expression of tight junctions of Caco-2 cells induced by inflammation and reduce the levels of TNF-a, IL-8, IL-1β, and IL-6, although they had no significant effect on the expression of iNOS and COX-2 mRNA induced by LPS. Meanwhile, MAPK and NF-κB signaling pathways play an important role in the LPS or TNF-α induced Caco-2 cell inflammation model. It has been reported that the metabolites of polyphenols could exert synergistic anti-inflammatory effects by downregulating MAPK and NF-κB signaling pathways in a TNF-α induced Caco-2 cell model (Zheng et al., 2021). In this case, the effect of RLD on the MAPK and NF-κB pathway in a TNF-α induced Caco-2 cell model are worth studying in future.

In order to simulate the real in vivo environment, Caco-2/RAW-264.7 co-culture model was further established to explore the anti-inflammation activity of RLD. Generally, the bioactives need to reach a certain concentration to exert its effects. Thus, the absorption and

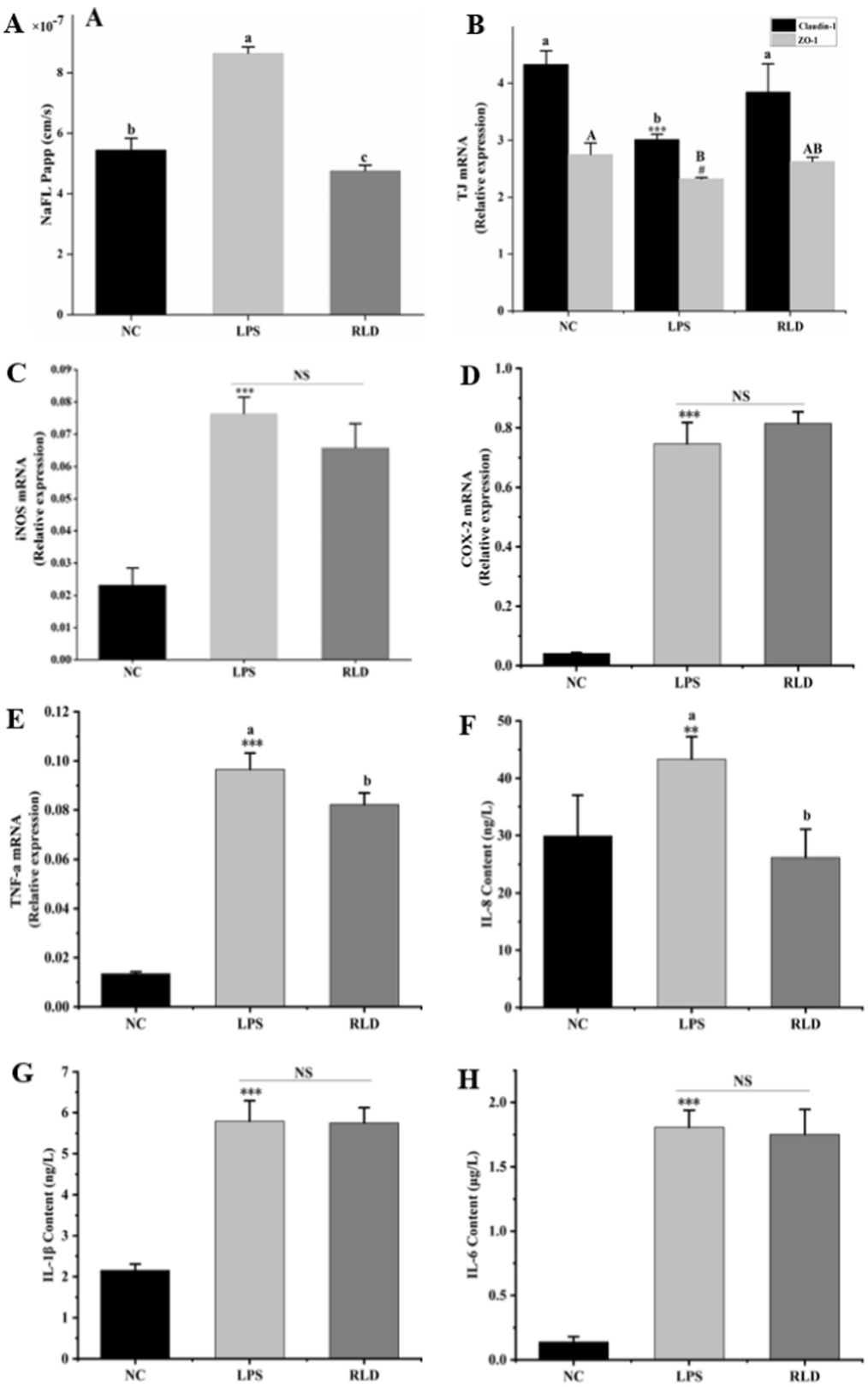

Fig. 6. Effect of RLD on intestinal barrier and intestinal inflammation in Caco-2/RAW264.7 co-culture. Papp value of fluorescein sodium in Caco-2 cell monolayer (A); the mRNA expression of claudin-1 and ZO-1 in Caco-2 cells (B); iNOS (C), COX-2 (D) and TNF-α (E) in RAW264.7 cells; IL-6 (H) and IL-1β (G) in the supernatant (BL side) of RAW264.7 cells; IL-8 (F) in the supernatant (AP side) of Caco-2 cells. The results were expressed as mean ± SD, n = 3. *: indicated the significant difference between the NC and LPS group, **: $P < 0.01$, ***: $P < 0.001$. Different letters represent significant difference between the LPS and experimental group ($P < 0.05$). NS means no significant difference.

transportation of RLD in the Caco-2 cell monolayer were previously investigated, results showed that only kaempferol tetraglucoside was transported into the basolateral (BL) side, which indicated that the finally in vivo concentrations of bioactives were much lower that of RLD we used within a reasonable range, but it still exhibited strong anti-inflammatory activity. Therefore, they do provide important insights into the anti-inflammatory effects of lentil hull polyphenols.

5. Conclusion

In conclusion, RLE and GLE exerted anti-inflammatory effects by inhibiting the activation of MAPK and NF-κB signaling pathways, and the effect of RLE was better. Meanwhile, after digestion by gastrointestinal tract, phenolic substances in the red lentil hulls are released continuously, and these digestive products can promote the expression of tight junction proteins, and be absorbed and transported to play a certain anti-inflammatory effect. These findings provide a theoretical basis for the development of lentil hulls and could be a potential functional dietary resource for the prevention of inflammatory diseases.

CRediT authorship contribution statement

Li Peng: Data curation, Investigation, Methodology, Software, Writing – original draft. **Fanghua Guo:** Data curation, Investigation, Methodology, Software, Writing – original draft. **Minjia Pei:** Data curation, Methodology, Writing – original draft. **Rong Tsao:** Supervision, Funding acquisition. **Xiaoya Wang:** Data curation, Formal analysis. **Li Jiang:** Validation, Visualization. **Yong Sun:** Conceptualization, Writing – review & editing, Funding acquisition. **Hua Xiong:** Conceptualization, Writing – review & editing, Funding acquisition.

Declaration of Competing Interest

The authors declare that they have no known competing financial interests or personal relationships that could have appeared to influence the work reported in this paper.

Acknowledgment

The authors thank Ms. Heather Hill of the Canadian International Grains Institute (CIGI) for providing the lentil hull samples. This project was financially supported by the A-base funding of Agriculture & Agri-Food Canada (AAFC) (Project # J-001322.001.04; PSS#2927), the Ontario Research fund (ORF) # RE-08-082, and the AAFC Collaborative Framework in collaboration with Saskatchewan Pulse Growers (# 40004678). This study was also supported by National Natural Science Foundation of China (# 82060781), China Postdoctoral Science Foundation (# 2020M671975) and the key project for science and technology research of Jiangxi province in 2018 (5511, 20182ABC28010).

Appendix A. Supplementary material

Supplementary data to this article can be found online at https://doi.org/10.1016/j.jff.2022.105044.

References

Bian, Y., Dong, Y., Sun, J., Sun, M., Hou, Q., Lai, Y., & Zhang, B. (2020). Protective effect of kaempferol on LPS-induced inflammation and barrier dysfunction in a coculture model of intestinal epithelial cells and intestinal microvascular endothelial cells. *Journal of Agriculture and Food Chemistry, 68*(1), 160–167. https://doi.org/10.1021/acs.jafc.9b06294

Blancas-Benitez, F. J., Pérez-Jiménez, J., Montalvo-González, E., González-Aguilar, G. A., & Sáyago-Ayerdi, S. G. (2018). In vitro evaluation of the kinetics of the release of phenolic compounds from guava (*Psidium guajava* L.) fruit. *Journal of Functional Foods, 43*, 139–145. https://doi.org/10.1016/j.jff.2018.02.011

Brodkorb, A., Egger, L., Alminger, M., Alvito, P., Assuncao, R., Ballance, S., … Recio, I. (2019). INFOGEST static in vitro simulation of gastrointestinal food digestion. *Nature Protocols, 14*(4), 991–1014. https://doi.org/10.1038/s41596-018-0119-1

Dinarello, C. A. (2011). A clinical perspective of IL-1β as the gatekeeper of inflammation. *European Journal of Immunology, 41*(5), 1203–1217. https://doi.org/10.1002/eji.201141550

Duenas, M., Hernandez, T., & Estrella, I. (2006). Assessment of in vitro antioxidant capacity of the seed coat and the cotyledon of legumes in relation to their phenolic contents. *Food Chemistry, 98*(1), 95–103. https://doi.org/10.1016/j.foodchem.2005.05.052

Herlaar, E., & Brown, Z. (1999). p38 MAPK signalling cascades in inflammatory disease. *Molecular Medicine, 5*.

Fang, H. Y., Chen, Y. K., Chen, H. H., Lin, S. Y., & Fang, Y. T. (2012). Immunomodulatory effects of feruloylated oligosaccharides from rice bran. *Food Chemistry, 134*(2), 836–840. https://doi.org/10.1016/j.foodchem.2012.02.190

Feng, M., Wang, X., Xiong, H., Qiu, T., Zhang, H., Guo, F., … Sun, Y. (2021). Anti-inflammatory effects of three selenium-enriched brown rice protein hydrolysates in LPS-induced RAW264.7 macrophages via NF-κB/MAPKs signaling pathways. *Journal of Functional Foods, 76*. https://doi.org/10.1016/j.jff.2020.104320

Guo, F., Xiong, H., Wang, X., Jiang, L., Yu, N., Hu, Z., … Tsao, R. (2019). Phenolics of green pea (*Pisum sativum* L.) hulls, their plasma and urinary metabolites, bioavailability, and in vivo antioxidant activities in a rat model. *Journal of Agriculture and Food Chemistry, 67*(43), 11955–11968. https://doi.org/10.1021/acs.jafc.9b04501

Han, B. H., Lee, Y. J., Yoon, J. J., Choi, E. S., Namgung, S., Jin, X. J., … Lee, H. S. (2017). Hwangryunhaedoktang exerts anti-inflammation on LPS-induced NO production by suppressing MAPK and NF-κB activation in RAW264.7 macrophages. *Journal of Integrative Medicine, 15*(4), 326–336. https://doi.org/10.1016/s2095-4964(17)60350-9

Hooshmand, S., Kumar, A., Zhang, J. Y., Johnson, S. A., Chai, S. C., & Arjmandi, B. H. (2015). Evidence for anti-inflammatory and antioxidative properties of dried plum polyphenols in macrophage RAW 264.7 cells. *Food & Function, 6*(5), 1719–1725. https://doi.org/10.1039/c5fo00173k

Hu, T. Y., Ju, J. M., Mo, L. H., Ma, L., Hu, W. H., You, R. R., … Cheng, B. H. (2019). Anti-inflammation action of xanthones from Swertia chirayita by regulating COX-2/NF-kappaB/MAPKs/Akt signaling pathways in RAW 264.7 macrophage cells. *Phytomedicine, 55*, 214–221. https://doi.org/10.1016/j.phymed.2018.08.001

Hu, X., Yu, Q., Hou, K., Ding, X., Chen, Y., Xie, J., … Xie, M. (2020). Regulatory effects of Ganoderma atrum polysaccharides on LPS-induced inflammatory macrophages model and intestinal-like Caco-2/macrophages co-culture inflammation model. *Food and Chemical Toxicology, 140*, Article 111321. https://doi.org/10.1016/j.fct.2020.111321

Jakobek, L., & Matić, P. (2019). Non-covalent dietary fiber-polyphenol interactions and their influence on polyphenol bioaccessibility. *Trends in Food Science & Technology, 83*, 235–247.

Kaminska, B. (2005). MAPK signalling pathways as molecular targets for anti-inflammatory therapy–from molecular mechanisms to therapeutic benefits. *Biochimica et Biophysica Acta, 1754*(1–2), 253–262. https://doi.org/10.1016/j.bbapap.2005.08.017

Kim, T. H., & Bae, J. S. (2010). Ecklonia cava extracts inhibit lipopolysaccharide induced inflammatory responses in human endothelial cells. *Food and Chemical Toxicology, 48*(6), 1682–1687. https://doi.org/10.1016/j.fct.2010.03.045

Li, L., Chen, J., Lin, L., Pan, G., Zhang, S., Chen, H., … You, Z. (2020). Quzhou Fructus Aurantii Extract suppresses inflammation via regulation of MAPK, NF-κB, and AMPK signaling pathway. *Scientific reports, 10*(1), 1–13.

Liu, C., Tang, X., Zhang, W., Li, G., Chen, Y., Guo, A., & Hu, C. (2019). 6-Bromoindirubin-3'-oxime suppresses LPS-induced inflammation via inhibition of the TLR4/NF-kappaB and TLR4/MAPK signaling pathways. *Inflammation, 42*(6), 2192–2204. https://doi.org/10.1007/s10753-019-01083-1

Maleki, S. J., Crespo, J. F., & Cabanillas, B. (2019). Anti-inflammatory effects of flavonoids. *Food Chemistry, 299*, Article 125124. https://doi.org/10.1016/j.foodchem.2019.125124

Maren Amasheh, Susanne Schlichter , Salah Amasheh, Joachim Mankertz, Martin Zeitz, Michael Fromm, & Schulzke, a. J. r. D. (2008). Quercetin Enhances Epithelial Barrier Function and Increases Claudin-4 Expression in Caco-2 Cells. *Nutrition and Disease, 138*, 1067–1073.

Marina, Z., Amin, I., Loh, S. P., Fadhilah, J., & Kartinee, K. N. (2019). Intestinal permeability and transport of apigenin across caco-2 cell monolayers. *Journal of Food Bioactives, 7*. https://doi.org/10.31665/jfb.2019.7198

Minjia, P., Xiaoya, W., Hua, X., Fengxin, W., & Yong, S. (2021). Analysis of Lentil Hulls Phenolics and Antioxidant Capacity Based on UPLC-ESI-QTOF-MS2. *Journal of Nanchang University*.

Mirali, M., Purves, R. W., & Vandenberg, A. (2017). Profiling the phenolic compounds of the four major seed coat types and their relation to color genes in lentil. *Journal of Natural Products, 80*(5), 1310–1317. https://doi.org/10.1021/acs.jnatprod.6b00872

Noda, S., Tanabe, S., & Suzuki, T. (2012). Differential effects of flavonoids on barrier integrity in human intestinal Caco-2 cells. *Journal of Agriculture and Food Chemistry, 60*(18), 4628–4633. https://doi.org/10.1021/jf300382h

Omonijo, F. A., Liu, S., Hui, Q., Zhang, H., Lahaye, L., Bodin, J. C., … Yang, C. (2019). Thymol improves barrier function and attenuates inflammatory responses in porcine intestinal epithelial cells during lipopolysaccharide (LPS)-induced inflammation. *Journal of Agriculture and Food Chemistry, 67*(2), 615–624. https://doi.org/10.1021/acs.jafc.8b05480

Oomah, B. D., Caspar, F., Malcolmson, L. J., & Bellido, A.-S. (2011). Phenolics and antioxidant activity of lentil and pea hulls. *Food Research International, 44*(1), 436–441. https://doi.org/10.1016/j.foodres.2010.09.027

Portman, D., Dolgow, C., Maharjan, P., Cork, S., Blanchard, C., Naiker, M., & Panozzo, J. F. (2020). Frost-affected lentil (*Lens culinaris* M.) compositional changes through extrusion: potential application for the food industry. *Cereal Chemistry, 97* (4), 818–826. https://doi.org/10.1002/cche.10296

Quirós-Sauceda, A., Palafox-Carlos, H., Sáyago-Ayerdi, S., Ayala-Zavala, J., Bello-Perez, L. A., Alvarez-Parrilla, E., … González-Aguilar, G. (2014). Dietary fiber and phenolic compounds as functional ingredients: Interaction and possible effect after ingestion. *Food & function, 5*(6), 1063–1072.

Sadeghi Ekbatan, S., Iskandar, M. M., Sleno, L., Sabally, K., Khairallah, J., Prakash, S., & Kubow, S. (2018). Absorption and metabolism of phenolics from digests of polyphenol-rich potato extracts using the Caco-2/HepG2 co-culture system. *Foods, 7* (1). https://doi.org/10.3390/foods7010008

Sun, Y., Deng, Z. Y., Liu, R. H., Zhang, H., Zhu, H. H., Jiang, L., & Tsao, R. (2020). A comprehensive profiling of free, conjugated and bound phenolics and lipophilic antioxidants in red and green lentil processing by-products. *Food Chemistry, 325*.

Sun, Y., Qin, Y., Li, H., Peng, H., Chen, H., Xie, H.-R., & Deng, Z. (2015). Rapid characterization of chemical constituents in Radix Tetrastigma, a functional herbal mixture, before and after metabolism and their antioxidant/antiproliferative activities. *Journal of Functional Foods, 18*, 300–318.

Troszyńska, A., Estrella, I., López-Amóres, M. L., & Hernández, T. (2002). Antioxidant activity of pea (*Pisum sativum* L.) seed coat acetone extract. *LWT - Food Science and Technology, 35*(2), 158–164. https://doi.org/10.1006/fstl.2001.0831

Villela-Castrejón, J., Antunes-Ricardo, M., & Gutiérrez-Uribe, J. A. (2017). Bioavailability and anti-inflammatory activity of phenolic acids found in spray-dried nejayote after its in vitro digestion. *Journal of Functional Foods, 39*, 37–43. https://doi.org/10.1016/j.jff.2017.09.058

Wang, X., Yu, N., Wang, Z., Qiu, T., Jiang, L., Zhu, X., … Xiong, H. (2020). Akebia trifoliata pericarp extract ameliorates inflammation through NF-kappaB/MAPK signaling pathways and modifies gut microbiota. *Food & Function, 11*(5), 4682–4696. https://doi.org/10.1039/c9fo02917f

Wang, Z., Li, S., Ge, S., & Lin, S. (2020). Review of distribution, extraction methods, and health benefits of bound phenolics in food plants. *Journal of Agricultural and Food Chemistry, 68*(11), 3330–3343.

Weiguang YI, Casimir C. Akoh, Joan Fischer, & Krewer, A. G. (2006). Absorption of Anthocyanins from Blueberry Extracts by Caco-2 Human Intestinal Cell Monolayers. *J. Agric. Food Chem, 54*, 5651−5658.

Yeo, J., & Shahidi, F. (2020). Identification and quantification of soluble and insoluble-bound phenolics in lentil hulls using HPLC-ESI-MS/MS and their antioxidant potential. *Food Chemistry, 315*, Article 126202. https://doi.org/10.1016/j.foodchem.2020.126202

Chen, Z.-B., Yu, Y.-B., Wa, Q.-B., Zhou, J.-W., He, M., & Cen, Y. (2020). The role of quinazoline in ameliorating intervertebral disc degeneration by inhibiting oxidative stress and anti-inflammation via NF-κB/MAPKs signaling pathway. *European Review for Medical and Pharmacological Sciences, 24*, 2077–2086.

Zelova, H., & Hosek, J. (2013). TNF-α signalling and inflammation: Interactions between old acquaintances. *Inflammation Research, 62*(7), 641–651. https://doi.org/10.1007/s00011-013-0633-0

Zhang, B., Deng, Z., Tang, Y., Chen, P., Liu, R., Ramdath, D. D., … Tsao, R. (2014). Fatty acid, carotenoid and tocopherol compositions of 20 Canadian lentil cultivars and synergistic contribution to antioxidant activities. *Food Chemistry, 161*, 296–304. https://doi.org/10.1016/j.foodchem.2014.04.014

Zhang, H., Hassan, Y. I., Liu, R., Mats, L., Yang, C., Liu, C., & Tsao, R. (2020). Molecular mechanisms underlying the absorption of aglycone and glycosidic flavonoids in a Caco-2 BBe1 cell model. *ACS Omega, 5*(19), 10782–10793.

Zheng, S., Zhang, H., Liu, R., Huang, C.-L., Li, H., Deng, Z.-Y., & Tsao, R. (2021). Do short chain fatty acids and phenolic metabolites of the gut have synergistic anti-inflammatory effects?–New insights from a TNF-α-induced Caco-2 cell model. *Food Research International, 139*, Article 109833.

Zhong, L., Fang, Z., Wahlqvist, M. L., & Wu, G. (2018). Seed coats of pulses as a food ingredient: Characterization, processing, and applications. *Trends in Food Science & Technology, 80*, 35–42.

Zhou, Q., Sun, H. J., Liu, S. M., Jiang, X. H., Wang, Q. Y., Zhang, S., & Yu, D. H. (2020). Anti-inflammation effects of the total saponin fraction from Dioscorea nipponica Makino on rats with gouty arthritis by influencing MAPK signalling pathway. *BMC Complementary Medicine and Therapies, 20*(1), 261. https://doi.org/10.1186/s12906-020-03055-7